

## COMPARISON OF THREE SEISMIC ANALYSIS MODELS OF STEEL PIPE SHEET PILE BRIDGE FOUNDATION

Nguyen Thanh TRUNG<sup>1</sup>, Osamu KIYOMIYA<sup>2</sup> and Tongxiang AN<sup>3</sup>

<sup>1</sup>Student member of JSCE, Doctoral student, Waseda University (〒169-8555 Tokyo, Shinjuku-ku, Okubo 3-4-1)

<sup>2</sup>Fellow member of JSCE, Professor, Waseda University (〒169-8555 Tokyo, Shinjuku-ku, Okubo 3-4-1)

<sup>3</sup>Member of JSCE, A. Professor, Waseda University (〒169-8555 Tokyo, Shinjuku-ku, Okubo 3-4-1)

### 1. INTRODUCTION

Steel Pipe Sheet Pile (SPSP) foundation has high bearing capacity and high construction reliability, even for the poor construction sites such as large water depth and/or soft surface ground can be adopted. Given the soil-structure interaction (SSI), the nonlinear properties of the soil and the interlocks between the pipes, the seismic behavior of SPSP foundation is very complex, and a large scale model is required in general to evaluate the seismic performance of SPSP foundation accurately.

In the current bridge seismic design specifications, the bridge substructure with a SPSP foundation is designed by separating the column of the pier from the top of the SPSP foundation and the column is assumed to be supported at its bottom by a couple of linear springs which stiffness is calculated on the SPSP foundation, and the SPSP foundation is modeled as an imaginary well beam considering the shear slippage of the joints supported by soil springs with nonlinear property for large scale earthquake. The seismic design loads for the SPSP foundation are taken as the reaction forces of the linear springs or the lateral strength of the pier column, i.e. the seismic SSI and the nonlinear properties of the structure are incompletely taken into account in the current seismic design approach.

In order to verify the effects of the SSI, nonlinear properties of the structure on the vibration behavior and seismic performance of substructure, dynamic analyses were conducted on three models in this study: 1) The pier column was supported by three concentrated springs that indicated the SPSP foundation; 2) The pier column was supported by a beam with soil springs and 3) The pier column was supported by a 2D frame with soil springs and joint springs. Dynamic analyses were carried out by time history direct integration method using large scale earthquake waves.

### 2. PROTOTYPE BRIDGE PIER FOUNDATION

A typical Steel Pipe Sheet Pile foundation and the bridge pier that was supporting as shown in Fig.1 were

considered in this work. The height of the pier column is 13 m and the sectional dimension of the pier column is 2.5 m x 7.5 m, the thickness of the footing is 4m. The pier column is constructed of RC, and the strength of the concrete is 30 MPa. The SPSP foundation has a circular shape in plan with an outside diameter of 12.145m. The steel pipe has a diameter of 1.0 m with a thickness of 0.012 m. The material of the steel pipe is SKY400. The interlocking has a diameter of 0.1652 m with a modulus of stiffness of 120000 kN/m<sup>2</sup> in longitudinal direction, a compressive modulus of stiffness of 500000 kN/m<sup>2</sup> in horizontal direction and a shear modulus of stiffness of 5000 kN/m<sup>2</sup> in horizontal direction.

The surface ground consists of four layers: the first layer is a clay layer with an average SPT value of 2, an adhesion of 200 kN/m<sup>2</sup> and the depth of 1 m. The second layer is also a clay layer with an average SPT value of 3, an adhesion of 300 kN/m<sup>2</sup> and the depth of 20.5 m. The third layer is a dense sand layer with an average SPT value of 20, an inner friction angle of 32 degrees and the depth of 3 m. The bearing layer is a gravel layer with an average SPT value of 50, an inner friction angle of 40 degrees and the depth of 1.5 m (as shown in Fig.1).

### 3. CALCULATION MODELS AND INPUT GROUND MOTIONS

#### 3.1. Calculation models

The analysis was carried out on three models in this work. The pier column was modeled as beam elements. As to Model 1, the SPSP foundation was modeled as concentrated springs, while the SPSP was modeled as beam elements and the soil was modeled as soil springs for Model 2 and Model 3. The stiffness of the soil springs was determined from the stiffness of the soil and SPSP according to Highway Bridge Design Specifications 2002 (JRA-2002).

(a) *Concentrated spring model (Mode 1)*: as shown in Fig.2, the SPSP foundation was modeled as three concentrated springs  $K_v$ ,  $K_h$  and  $K_r$  in the horizontal, vertical and rotational direction, respectively.

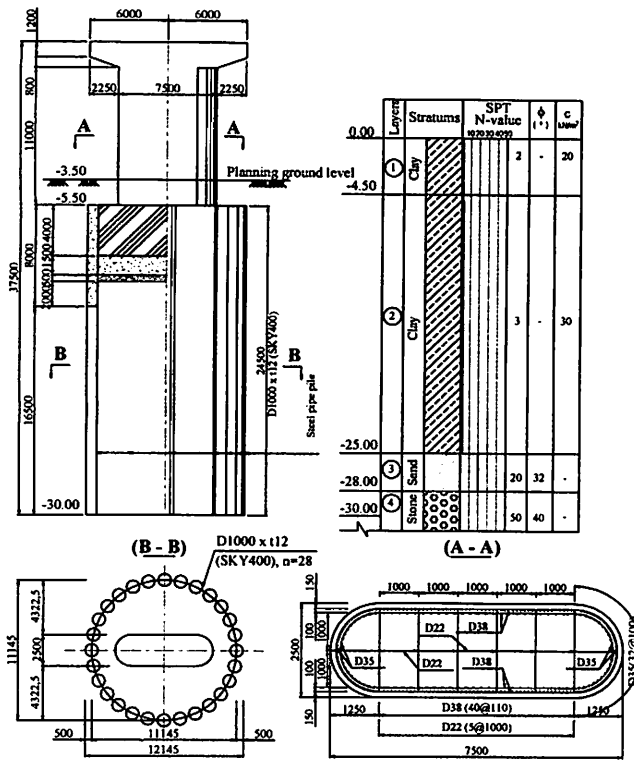


Figure -1 Prototype bridge pier with Steel Pipe Sheet Pile, foundation and soil properties

The pier column and top slab was supported by these three springs whose stiffness was calculated as follows:

$$K = F\delta^{-1} \quad (1)$$

Where,  $K$ : the stiffness matrix of springs;  $\delta$ : the displacement matrix at the bottom of footing. The stiffness of soil surrounding the footing was modeled in the horizontal,  $K_{th}$ , and in the vertical,  $K_{fv}$ .

(b) *One column with soil spring model (Model 2)*: as shown in Fig.3, the SPSP foundation was modeled as one column supported by soil springs that represented the function of the soil, and the pier column and top slab were supported by this column. The foundation column was divided into 15 segments in its axial direction. The flexural rigidity of this beam was derived by:

$$E_S I_z = E_S \left( \sum_{i=1}^{n_1+n_2} I_{oi} + \mu \sum_{i=1}^{n_1+n_2} A_{oi} x_i^2 \right) \quad (2)$$

Where,  $I_z$ : second moment of area of steel pipe sheet pile foundation ( $m^4$ );  $E_S$ : Young's modulus of steel pipe pile foundation ( $kN/m^2$ );  $A_{oi}$ : net cross-sectional area of  $i^{th}$  steel pipe body ( $m^2$ );  $I_{oi}$ : second moment of area of  $i^{th}$  steel pipe sheet pile and inner single pile ( $m^4$ );  $\mu$ : composite efficiency ( $=0.75$ );  $x_i$ : the distance from centroid of  $i^{th}$  steel pipe sheet pile and inner single pile to neutral axis in horizontal section of foundation ( $m$ );  $n_1$ : number of steel pipe sheet piles at periphery of well part (pile);  $n_2$ : number of steel pipe sheet piles in bulkhead (pile). The surrounding soil was represented by 15 couple of concentrated springs:  $K_{th}$  in horizontal direction and  $K_{fv}$  in vertical direction ( $i$ :  $i^{th}$  soil layer) were derived by:

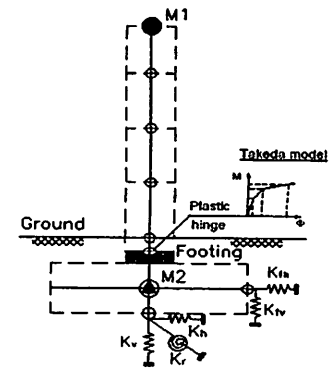


Figure -2 A column model with concentrated spring (Model 1)

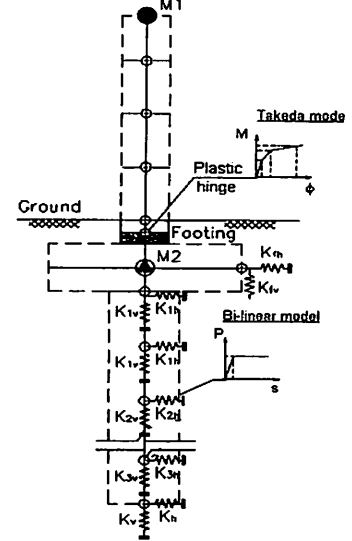


Figure -3 A column model with soil springs (Model 2)

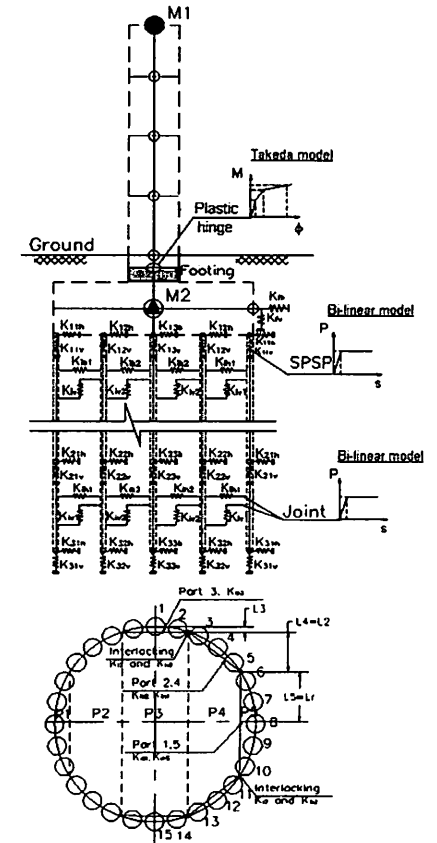


Figure -4 2D frame model with soil springs (Model3)

$$K_{ih} = D l_r k_{hi} \quad (3)$$

$$K_{iv} = D l_r k_{vi} \quad (4)$$

Where,  $D$ : the outside diameter of foundation (m),  $l_r$ : the length of  $r^{th}$  segment (m),  $k_{hi}$ : the coefficient of reaction of  $i^{th}$  soil layer in the horizontal and vertical direction ( $\text{kN/m}^3$ ). They were determined following JRA-2002.

(c) *2D frame with soil spring model (Model3)*: as shown in Fig.4, the SPSP was divided into five parts with equal width in horizontal direction in plan, and each part was represented by a beam at its center. Each beam was supported by 15 couple of concentrated soil springs ( $K_{ihj}$ ,  $K_{ivj}$ ) ( $i$ : the  $i^{th}$  soil layer,  $j$ : the  $j^{th}$  beam,  $j \in \{1,5\}$ ) whose stiffness were derived by:

$$K_{ihi} = L_i l_r k_{hi} \quad (5)$$

$$K_{ivi} = L_i l_r k_{vi} \quad (6)$$

Where,  $L_j$ : the length of the  $j^{th}$  part (m);  $l_r$ : the length of the  $r^{th}$  segment (m);  $k_{hi}$ ,  $k_{vi}$ : the coefficients of reaction of the  $i^{th}$  soil layer in the horizontal and vertical direction determined in JRA-2002 ( $\text{kN/m}^3$ ). Adjacent beams were jointed with each other by 15 couple of concentrated springs, ( $K_{lhi}$ ,  $K_{lvi}$ ) ( $i:1,2$ ) which have the stiffness were determined from the relationship between the shear capacity and the displacement of site experiment. The stiffness of spring  $K_{lvi}$  is a compressive modulus in longitude direction of pile. Regard to the stiffness of spring  $K_{lhi}$  in the horizontal direction was derived by:

$$K_{lhi} = L_i (K_c \cos \theta_j + K_s \sin \theta_j) \quad (7)$$

Where,  $L_j$ : the length of the  $j^{th}$  part (m);  $K_c$ : compressive modulus of  $j^{th}$  interlocking part ( $\text{kN/m}^2$ );  $K_s$ : shear modulus of stiffness of  $j^{th}$  interlocking part ( $\text{kN/m}^2$ );  $\theta_j$ : the angle between the horizontal axis and tangent axis at the point of  $j^{th}$  interlocking part (rad).

### 3.2. Input ground motions

The selected time history ground motion had a mean acceleration response spectrum comparing with the design response spectra proposed by JRA 2002 for type 2 of level 2 ground motion, as shown in Fig.5. It named JMA KOB wave with the peak acceleration of 812 Gal and lasting time of 30s.

Two types of ground motion input were considered in this study. One was earthquake acceleration uniform input and the other was multi-point forced displacement input. To obtain the surface ground amplitude along the depth of the soil layers to the selected ground motion, the ground dynamic analysis was conducted by inputting the JMA KOB wave at the bottom of the base layer. Soil Plus program was available in this calculation. The time histories were applied to the respective soil springs of considered models.

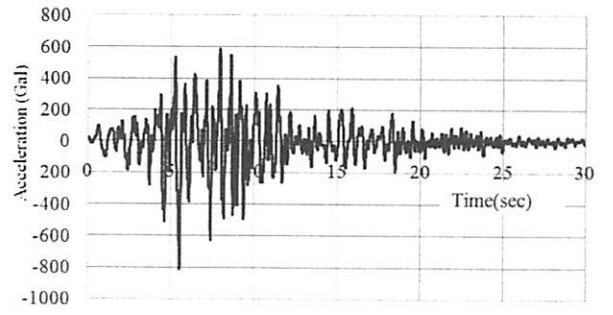


Figure -5 JMA KOB acceleration wave

## 4. MODELLING METHODOLOGY AND VERIFICATION PROCEDURE

The nonlinear dynamic analysis was conducted by time history direct integration method on three models. TDAP III program was available in this study. The hysteretic behavior of plastic hinge of the pier column was considered by Takeda model in all three models. The soil springs and interlocking springs were considered by bilinear model for nonlinear models. The upper limits of ground resistance were calculated according to JRA 2002 and upper limits of interlocking springs were calculated according to compression, tension, shear tests of interlocking, the details of these tests are shown in the reference. The damping ratio of structure and soil springs was assumed to be 0.03 and 0.15, respectively. Rayleigh's damping was used in this work.

To verify the effects of the nonlinear properties of the structure on the vibration behavior and seismic performance of the substructure, the analysis was carried out on nine cases (as shown in Table 1). Case 1c, case 2c and case 3c were conducted by multi-point forced displacement input (ID) and other cases were conducted by uniform earthquake acceleration input (IA). As to case 1a, case 2a and case 3a, the ground resistance and interlocking behavior were linear for Model 1, Model 2 and Model 3, respectively. As to case 1b, the concentrated springs was assumed to be nonlinear for Model 1 which properties were determined by the  $P-\delta$  curve from case 3b. The  $P-\delta$  curve was obtained from the push over analysis. For case 2b and case 2c of model 2, ground resistance behavior was bilinear and equivalent composite efficiency was considered by Eq.(2). The efficiency coefficient  $\mu$  was 0.84 that was determined by the nonlinear static analysis on model 3. As to case 3b and case 3c, the ground resistance and interlocking behavior worked as bilinear model.

It was thought the results of case 3b and case 3c were closer to the real performance of the structure, comparing with the results of the other cases to investigate the similarities and differences and verify the reasonableness of the models and the effect of nonlinear properties.

**Table -1** Analytical cases

No	Analytical cases	Model	Ground property	Interlocking property	Input type
1	Case 1a	Model 1	Linear	-	IA
2	Case 1b		Equivalent		IA
3	Case 1c		Equivalent		ID
4	Case 2a	Model 2	Linear	-	IA
5	Case 2b		Bilinear	Equivalent	IA
6	Case 2c		Bilinear	Equivalent	ID
7	Case 3a	Model 3	Linear	Linear	IA
8	Case 3b		Bilinear	Bilinear	IA
9	Case 3c		Bilinear	Bilinear	ID

Note:

1. IA: Uniform acceleration input
2. ID: Multi point forced displacement input.

**Table -2** Results of Eigen - value Analysis

Mode No	Model	Frequency (Hz)	Mode damping (%)	Mass ratio (%)
First mode	Model 1	2.10	8.27	43
	Model 2	2.07	6.05	63
	Model 3	2.14	5.72	54
Second mode	Model 1	4.95	11.22	44
	Model 2	6.49	9.89	33
	Model 3	5.16	9.42	43

**5. EIGEN-VALUE ANALYSIS**

As an example, the results in longitudinal direction of the bridge (the direction X) were introduced here. The frequency, mode damping and effective mass ratio were shown in Table 2.

The natural frequency ratio of Model 1, Model 2 and Model 3 was 1.00:0.98:1.02 respectively. The natural frequency of Model 2 was smallest. Because flexural rigidity of SPSP foundation was calculated by using composite efficiency of 0.75, while the equivalent composite efficiency calculated by Model 3 was 0.84. Regard as mode damping, Model 3 was the smallest and the ratio with Model 1, Model 2 was 1.00:1.45:1.06 for mode 1 and 1.00:1.19:1.05 for mode 2. It was thought that the damping ratio 0.03 of SPSP in Model 2 and Model 3 makes a decrease of damping ratios of entire structure.

**6. VIBRATION BEHAVIOR**

The vibration behavior of the structure was verified based on the acceleration and displacement responses of the superstructure. The displacement time history

**Table -3** Maximum displacement and acceleration

No	Analytical case	Disp. of the superstr. (m)	Disp. at the top of footing (m)	Acc. of the superstr. (m/s <sup>2</sup> )
1	Case 1a	0.118	0.018	10.8
2	Case 1b	0.146	0.048	11.1
3	Case 1c	0.393	0.262	10.4
4	Case 2a	0.129	0.020	10.9
5	Case 2b	0.158	0.053	8.5
6	Case 2c	0.385	0.223	11.3
7	Case 3a	0.143	0.038	11.7
8	Case 3b	0.168	0.067	9.7
9	Case 3c	0.414	0.273	10.9

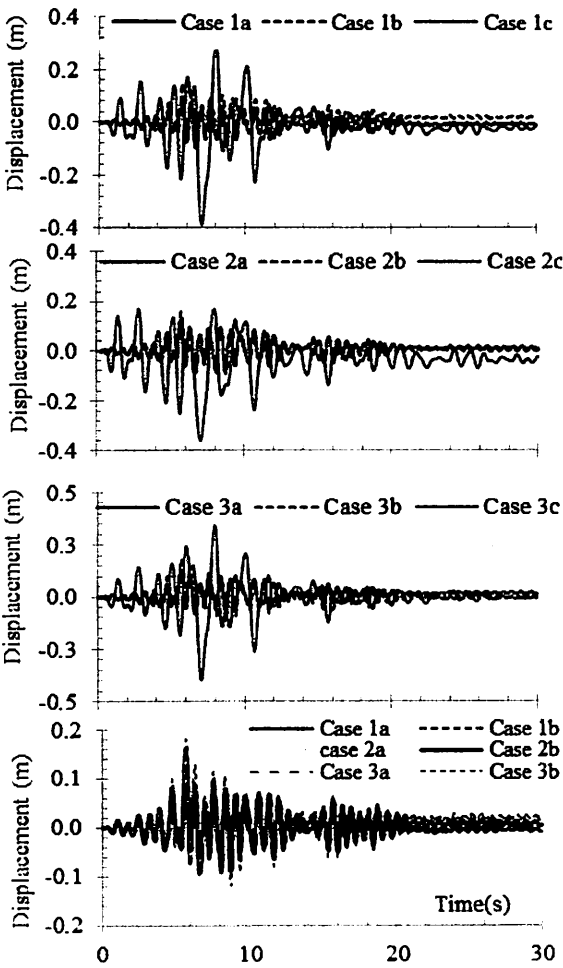


**Figure -6** Time histories of displacement response

responses were shown in Fig.6. The maximum displacement and maximum acceleration from the three models were shown in Table 3. As to case 1b, case 1a and case 1c, the ratio of the maximum displacement and that of the maximum acceleration were 1.00:0.84:2.69 and 1.00:0.97:0.96, respectively. For case 2b, case 2a and case 2c, the ratios were 1.00:0.86:2.44 of displacement and 1.00:1.06:1.32 of acceleration. For case 3b, case 3a

Table -4 Response ductility ratio and residual displacement

No	Analytical case	Maximum disp. at the top of pier(m)	Maximum response ductility ratio	Residual displacement (cm)
1	Case 1a	0.100	1.75	2.58
2	Case 1b	0.098	1.72	2.46
3	Case 1c	0.131	2.30	4.44
4	Case 2a	0.109	1.91	3.12
5	Case 2b	0.105	1.84	2.88
6	Case 2c	0.162	2.84	6.30
7	Case 3a	0.105	1.84	2.88
8	Case 3b	0.101	1.77	2.64
9	Case 3c	0.141	2.47	5.04

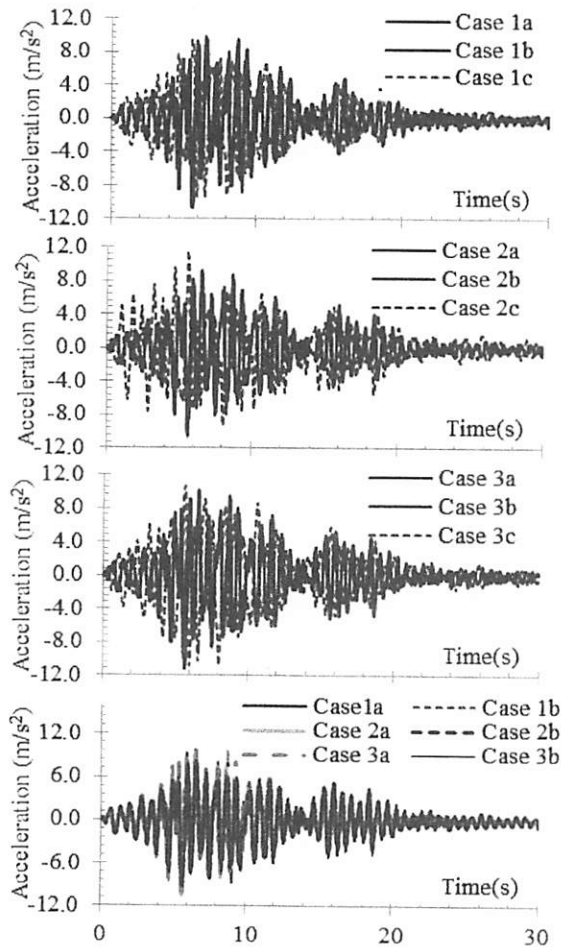


Figure -7 Acceleration response at the top of pier

and case 3c, the ratios were 1.00:0.84:2.45 of displacement and 1.00:1.05:1.12 of acceleration. The maximum displacement caused by IA from the cases with linear properties was smaller than that from the cases with nonlinear properties by 0.84-0.86 times and the maximum acceleration was affected by the nonlinear properties of the SPSP foundation. The maximum displacement caused by ID was bigger than that by IA by approximately 2.4-2.7 times. Comparing with case 3b, the maximum acceleration of case 1b was bigger by 14% but that of case 2b was smaller by 12%, the maximum

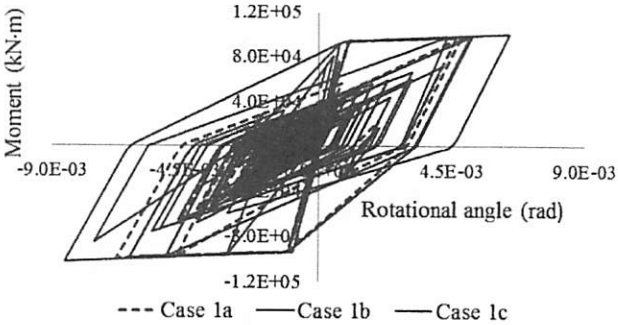


Figure -8 Hysteresis loop of bending moment against rotational angle of Case 1

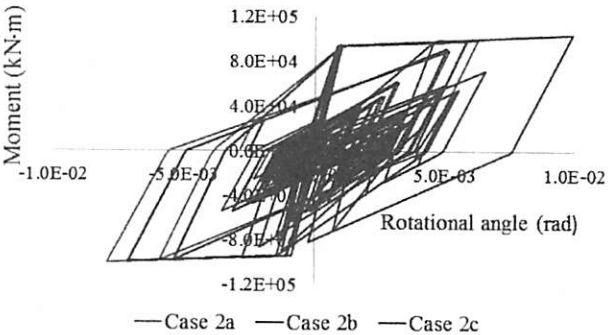


Figure -9 Hysteresis loop of bending moment against rotational angle of case 2

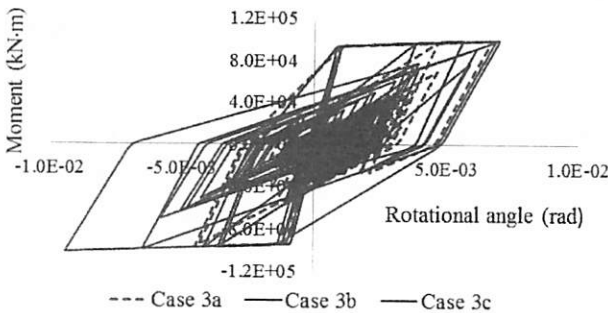


Figure -10 Hysteresis loop of bending moment against rotational angle of case 3

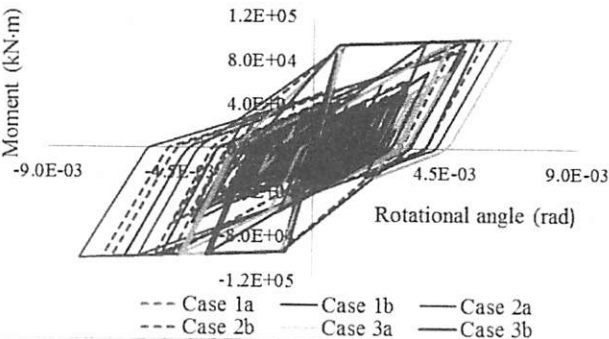


Figure -11 Hysteresis loop of bending moment against rotational angle

displacement of case 1b and case 2b was a bit smaller, their ratio was 1.00:0.88:0.94.Among the three models, Model 1 was the simplest. The response of the super-structure from case 1b was not so large different from the

case 3b, i.e. the maximum response of the superstructure was able to be roughly estimated by Model 1.

## 7. SEISMIC PERFORMANCE

The seismic performance of the structure was verified based on dynamic response of the pier column. The hysteresis loops of the bending moment against the rotational angle of the plastic hinge were shown in Fig.8, Fig.9, Fig.10 and Fig.11.

The maximum rotational angles of the case 1b, case 1a and case 1c were 6.31 mrad, 6.44 mrad and 8.76 mrad respectively, the ratio among them was 1.00:1.04:1.36 respectively. The rotational angles of case 2b, case 2a and case 2c were respectively 6.58 mrad, 7.11 mrad and 9.9 mrad and their ratio was 1.00:1.09:1.63 respectively. As to case 3b, case 3a and case 3c, the rotational angles respectively were 6.47 mrad, 6.71 mrad and 9.50 mrad and their ratio was 1.00:1.04:1.55 respectively. Based on the above ratios, regard to the case of IA ground motion the rotational angle of linear cases was larger than that nonlinear cases and the rotational angle of three models under ID ground motion was larger than that of them under IA ground motion. Therefore, the nonlinear properties of the SPSP foundation make a decrease of the rotational angle of the plastic hinge. Conversely, Multi point forced displacement input makes an increase of rotational angle and the difference between IA and ID was considerable. Comparing with case 3b, the rotational angle of case 1b was 2% smaller, while that of case 2b was 2% larger, i.e. Model 1 and Model 2 were able to estimate the maximum rotational angle of the plastic hinge.

The residual displacement  $\delta_R$  and the maximum response ductility ratio  $\mu$ , as shown in Table 4 were derived according to JRA 2002. As to the ratio of ductility, among case 1b, case 1a and case 1c was 1.00:1.05:1.81. For case 2b, case 2a and case 2c, the ratio was 1.00:1.04:2.19, and that for case 3b, case 3a and 3c, was 1.00:1.09:1.91. The above ratios showed that the residual displacement from the cases of SPSP foundation with linear properties was smaller than that from the cases of SPSP foundation with nonlinear properties and the ID ground motion increased the residual displacement approximately 2 times. Comparing with case 3b, the residual displacement of case 1b was 7% smaller, while that of case 2b was 9% larger, i.e. Model 1 and Model 2 were able to roughly estimate the residual displacement of the superstructure.

## 8. CONCLUSION

The vibration behavior and seismic performance of Steel Pipe Sheet Pile foundation were verified on three models by nonlinear dynamic analysis method in this study. The main findings are as following:

- 1) The nonlinear properties of the SPSP foundation increase the response displacement of the superstructure but decrease the rotational angle of the plastic hinge and residual displacement of the superstructure.
- 2) Multi point forced displacement input Earthquake displacement ground motion with amplitude variation along the depth of the soil layers makes a large increase of the response of the superstructure, the rotational angle of the plastic hinge and the residual displacement of the superstructure.
- 3) The 2D frame with soil spring model can directly take into account the nonlinear properties of the SPSP foundation and calculate a closer real result but is somewhat complex, while the Model 1 is relatively simple and can roughly estimate the vibration behavior and seismic performance of the structure even for the nonlinear cases.

## REFERENCE

- 1) JRA-2002. Specification for Highway Bridge, part V: *Seismic Design*, Japan Road Association, and part IV: *Substructure*, Japan Road Association, 2002.
- 2) Trung N.T. and Kiyomiya O. : Response analysis of steel pipe sheet pile foundation by three simple models. *Proceeding of the 39 Conference of JSCE*, Kanto Branch, March, 2011.
- 3) An T.X., Kiyomiya O. Hung T. V. and Kochi R: Nonlinear dynamic analysis of soil-steel pipe pile sheet-structure interaction under seismic excitation, *Proceedings of the 35<sup>th</sup> International Symposium on Bridge and Structural Engineering*, jointly organized by IABSE-IASS, London, UK, 2011.
- 4) Liam Finn W.D. Aspects of soil structure interaction, *Soil-Foundation-Structure Interaction* – Orense, Chouw & Pender, Taylor & Francis Group, London, ISBN 978-0-415-60040-8, pp 69-75, 2010.
- 5) Fumio Shima and Yasuhiko Ueki: Design method of three dimensional frame of Steel pipe sheet pile by well method, 2010.